CHAPTER IV

RESULTS AND DISCUSSION

4.1 Preparation and Characterization of Patterned PAA Brushes Having AuNPs

Water contact angle measurement was used as a tool to monitor the success of stepwise surface modification of the glass substrate. The data are expressed in terms of advancing/receding contact angle (θ_A/θ_R) as shown in Table 4.1. An extremely hydrophilic glass substrate having generated silanol groups after cleaning by plasma treatment ($\theta_A \sim 0$) became hydrophobic after reacting with APTES and yielded Si-NH_2. The substrate turned slightly less hydrophobic when being immobilized with initiator via the reaction with 4,4-azobis(4-cyanovaleic acid) (ACVA). Upon surface-initiated RAFT polymerization, the water contact of the glass substrate was further decreased to 16.6° implying that hydrophilic PAA brushes was grafted onto the surface. In contrast, the glass surface was highly hydrophobic with contact angles of 127.6°/74.5° after being modified with perfluorooctylsilyl group.

Table 4.1 Water contact angles of the glass substrate after stepwise modification

Surface Functionality	θ_A	θ_R
Si-OH	0	N/A
Si-NH_2	84.7 ± 5.7	52.1 ± 2.6
Si-initiator	75.8 ± 2.9	46.6 ± 6.3
Si-O-Si-PAA	16.6 ± 4.3	N/A
Si-O-Si-$(CH_2)_2(CF_2)_5CF_3$	127.6 ± 2.7	74.5 ± 4.3

N/A: Not measurable

Molecular weight ($\overline{M}_n$) and functional group of PAA simultaneously formed in solution from the "added" initiator were determined by ^{1}H NMR analysis. As depicted in Figure 4.1. The characteristic ^{1}H NMR peaks of the methylene proton in the AA unit (-CH(COOH)) and those aromatic protons of the dithiobenzoate group at the chain end of PAA appeared at 2.1-2.3 and 7.2-7.9 ppm, respectively. The average M_n of PAA was calculated from the relative ratio between the peak integration of proton from the PAA backbone and the peak integration of protons from the dithiobenzoate groups using eqn. 4.1. The fact that the calculated M_n of 6,005 g/mol closely resembled the anticipated value (7,206 g/mol) for the target degree of polymerization (DP) of 100 suggested that the RAFT process was well controlled.

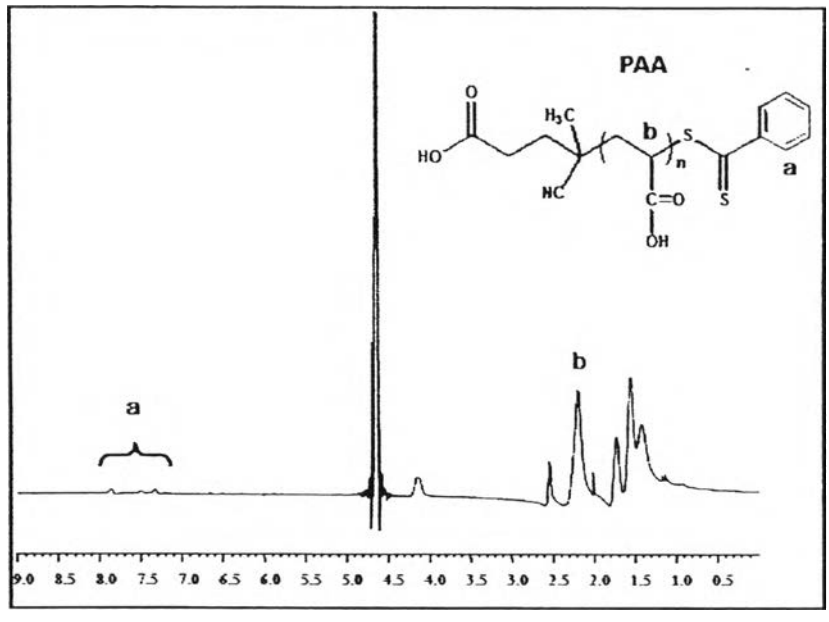

Figure 4.1 1H NMR spectra of PAA in solution

$$\text{Average } M_n = \left\{ \frac{\text{intergral of the } H_b \times M_{n\,(\text{acrylic acid})}}{\left(\frac{\text{intergral of the } H_a}{5} \right)} \right\} + M_{n\,(\text{CTA})} \qquad (4.1)$$

$M_{n(\text{acrylic acid})}$ = 72.06 g/mol, $M_{n(\text{CTA})}$ = 279.38 g/mol

The success of PAA surface grafting was confirmed by FT-IR analysis of silica particles grafted with PAA brushes. Figure 4.2(c) reveals characteristic absorption bands of C=O stretching at 1635 cm^{-1}(Amide I), N-H bending at 1562 cm^{-1}(Amide II) suggesting that amide linkage has been formed between the terminal amino groups of APTES and carboxyl groups of the initiator, ACVA. Strong signal of C=O stretching of carboxylic acid apparently emerged at 1718 cm^{-1} after surface-initiated RAFT polymerization took place as an indication of PAA brushes formation as shown in Figure 4.2(d).

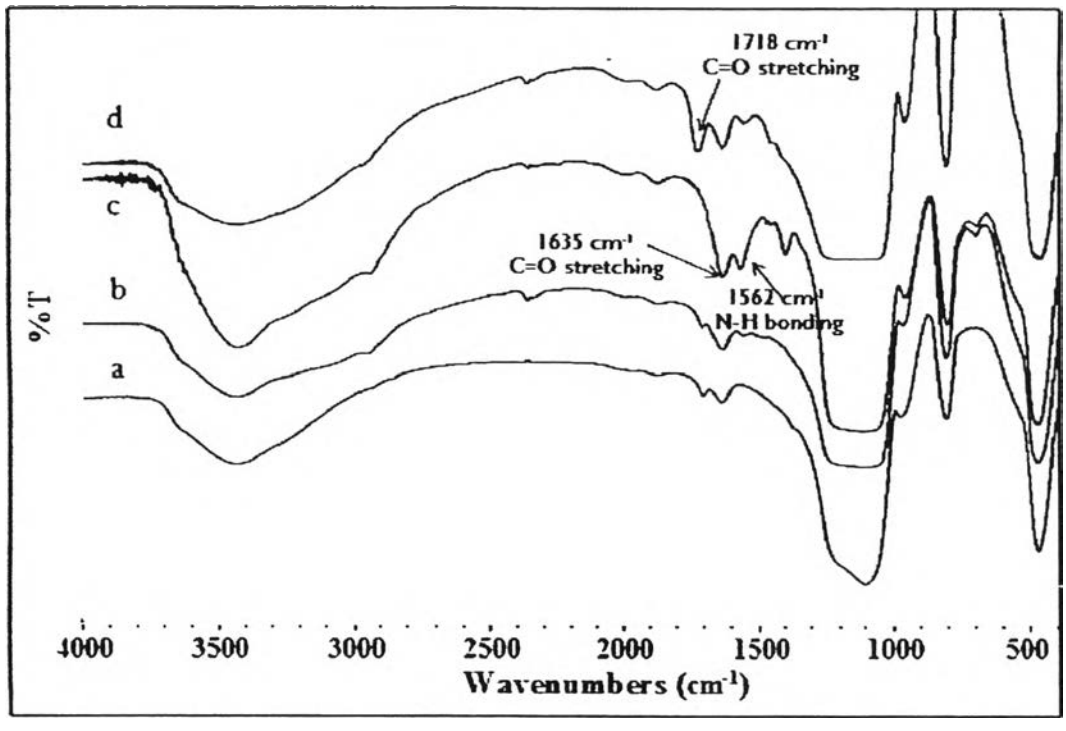

Figure 4.2 FT-IR spectra of (a) Si-OH (b) Si-APTES (c) Si-Initiator (d) Si-PAA.

A number of alternate dipping cycle in between $HAuCl_4$ solution and deionized water was varied to determine its effect on AuNPs formation on the PAA-modified glass substrate. As shown in Figure 4.3, the substrate became slightly darker upon increasing the number of cycle from 1 to 5 implying that there was greater amount of AuNPs as a function of dipping cycle. This may be explained as a consequence of pH-dependent conformational change of PAA. Because pKa of PAA is 4.2, PAA chains would adopt extended conformation when being soaked in DI water, having pH of approximately 6.0, due to ionic repulsion of the carboxylate groups along the chains. Once the PAA-modified surface was immersed in $HAuCl_4$ solution, having pH of 1.7, some carboxylate groups of the PAA chains should electrostatically interact with Au^{3+} and subsequently reduce it to Au^0. At the same time, the rest of

carboxylate groups were protonated and became less extended and more coil-like ,therefore can trap both Au^{3+} as well as the generated Au^{0} [32]. By repetitive performing this cycle of dipping, the more Au^{3+} can associate with the carboxylate groups and the more Au^{0} can be generated. Nevertheless, more quantitative data from ICP-MS analysis is necessary to verify this assumption.

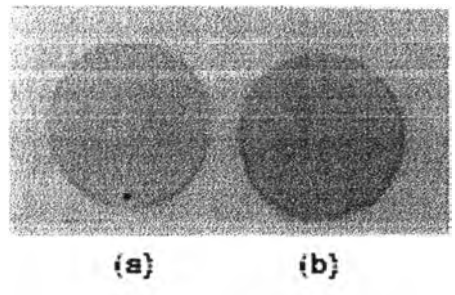

Figure 4.3 PAA-modified glass slide containing AuNPs generated by (a) 1 cycle of dipping and (b) 5 cycles of dipping in between 1 mM $HAuCl_4$ solution and deionized water.

Formation of AuNPs within the matrix of PAA brushes can be demonstrated in Figure 4.4. The area covered with UV-sensitive resist after surface patterning by photolithography (Step II in Scheme 3.1) can be seen as bright yellow spots in Figure 4.4a. After surface grafting of PAA brushes, the greater hydrophilicity of the PAA brushes than the surrounding area can be demonstrated by the ability to sustain water droplets as demonstrated in Figure 4.4b. Subsequent AuNPs formation within the PAA brushes can be visualized as dark spots on the glass substrate appearing in Figure 4.4c at the same positions as those previously covered with UV-sensitive resist in Figure 4.4a and water droplets in Figure 4.4b. This also suggests that carboxyl groups of PAA can act as effective reducing moieties for Au^{3+} leading to the

formation of AuNPs. This would add simplicity to the method because the reduction can be done without having to use additional reducing agent.

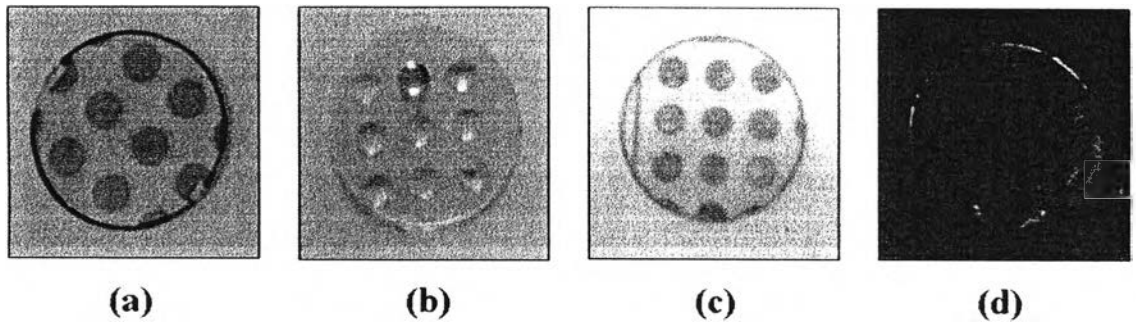

Figure 4.4 Patterned glass slide: covered with (a) positive UV-sensitive resist after photolithography step, (b) PAA brushes holding water droplets demonstrating their higher hydrophilicity than the surrounding area, (c) PAA brushes having *in situ* generated AuNPs, and (d) pattern used for photolithography.

The AuNPs immobilized on the PAA brushes was digested by aqua regia and later quantified by ICP-MS employing a calibration curve ($y=4\times10^{6}x-539.39$, $R^2=0.978$) shown in Figure 4.5. The content of AuNPs was found to be 2.46×10^{-9} mol/cm^2

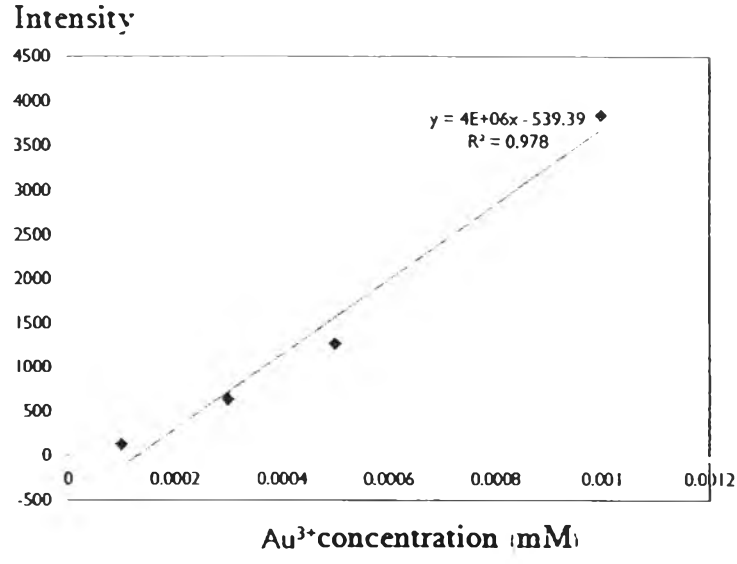

Figure 4.5 Calibration curve for Au^{3+} quantification by ICP-MS.

Morphology of the immobilized AuNPs on the glass substrate was determined by TEM. As can be seen in Figure 4.6, the AuNPs existed both in the form of well dispersed spherical particles with an average size of 18.45±2.34 nm (Figure 4.6a) and aggregated particles (Figure 4.6b). The aggregation is not unexpected given the fact that no stabilizer has been used in the AuNPs synthesis.

The presence of AuNPs on the PAA-modified glass surface was verified by XPS measurement (take-off angle of 90°). Figure 4.7 shows XPS spectra of the PAA-modified glass surface both before (a) and after (b) AuNPs immobilization. As shown in Figure 4.7(b), besides the signals of carbon (C_{1s}, binding energy of 287 eV) and oxygen (O_{1s}, binding energy of 533 eV) of PAA, a trace signal of gold (Au_{4f}) at binding energy of 84 eV was also observed implying the success of *in situ* synthesis of AuNPs on PAA brushes modified on glass substrate with 0.27% composition. It should also be emphasized that the ratio of C:O of 3:2 matched very well with the theoretical

value estimated from the repeat unit of AA unit (-CH_2CCOOH-). Percentages of elemental composition of all samples are shown in Table 4.2.

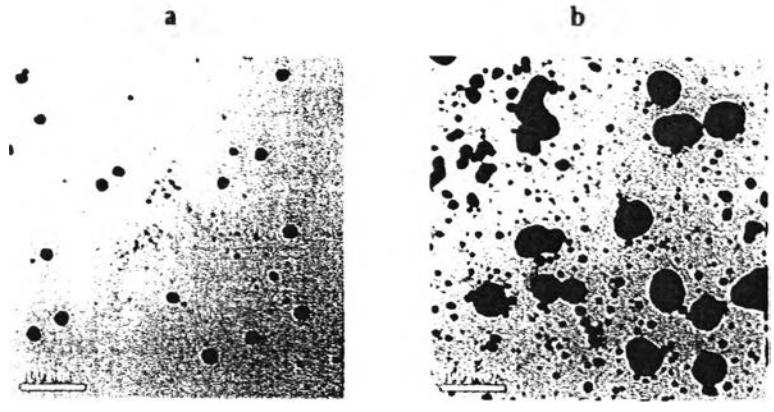

Figure 4.6 TEM images of AuNPs immobilized on PAA-modified glass substrate: (a) well dispersed particles and (b) aggregated particles.

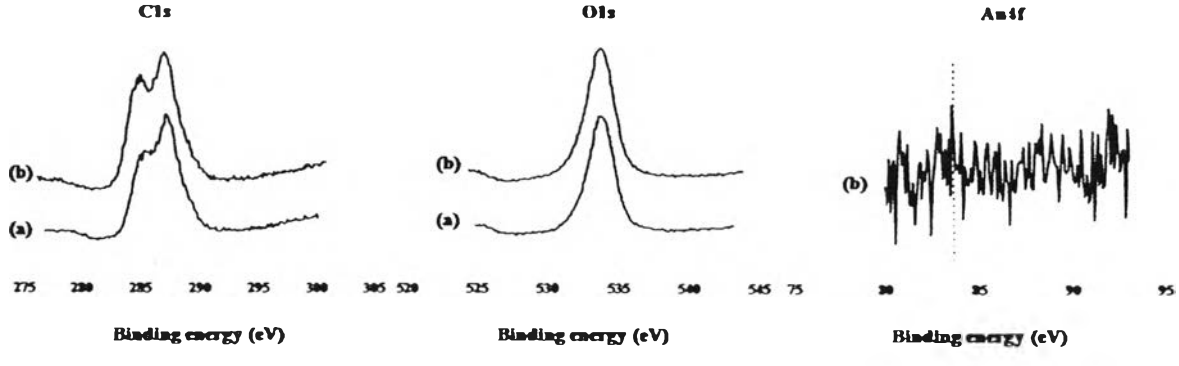

Figure 4.7 XPS spectra of (a) PAA-modified glass substrate and (b) PAA-modified glass substrate containing AuNPs.

Table 4.2 Percentage of elemental composition of PAA-modified glass surface both before and after AuNPs immobilization.

Element	PAA-modified glass surface (%)	PAA-modified glass surface containing AuNPs (%)
C_{1s}	40.35	40.92
O_{1s}	59.65	58.84
Au_{4f}	-	0.27

4.2 SALDI-MS analysis of Peptides on AuNPs-PAA Substrate

To determine the applicability of the PAA-modified glass substrate immobilized with AuNPs (AuNPs-PAA) as substrate for SALDI-MS analysis, bradykinin (MW 1060.21 g/mol)) was chosen as a standard peptide for analysis in comparison with the use of citrate-stabilized AuNPs as a MALDI matrix. As illustrated in Figure 4.8a, the citrate-stabilized AuNPs alone gave such a high background signal particularly in a mass range below m/z of 1,000 which is probably caused by partial ionization of the AuNPs. Therefore, poor signal of bradykinin was detected with relatively strong background when the analysis was done in the presence of citrate-stabilized AuNPs as can be seen in Figure 4.8b. On the other hand, a characteristic peak of bradykinin at m/z of 1060 was clearly observed without signal interference from AuNPs when the analysis was performed on a spot of PAA brushes containing AuNPs (Figure 4.8c). This result strongly indicated that the PAA brushes effectively

trapped and prevented the AuNPs from coming off the substrate so that their ionization was suppressed. The fact that the ion abundance of bradykinin was relatively high in Figure 4.8c suggested that the ionization efficiency was also improved perhaps by a better distribution of AuNPs within the matrix of PAA and PAA itself being a good proton source.

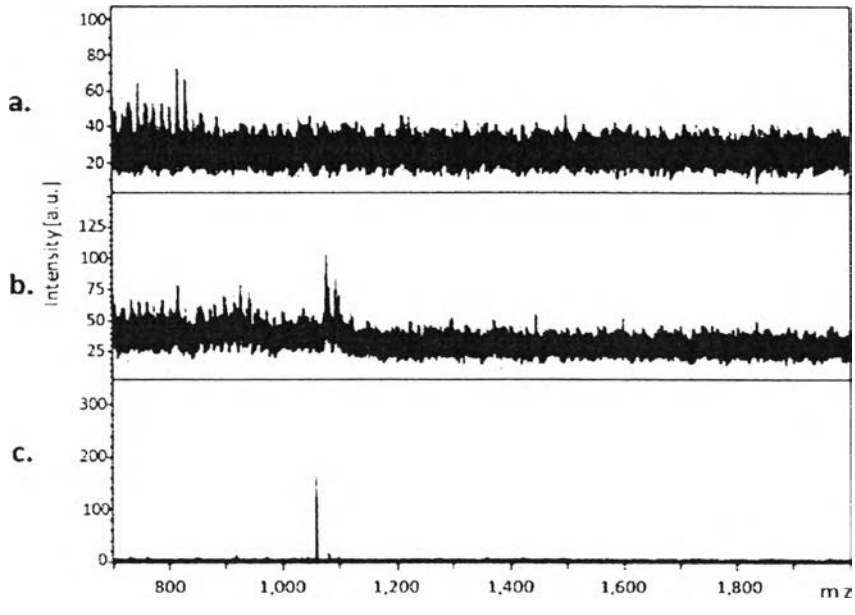

Figure 4.8 Mass spectra of (a) AuNPs, (b) bradykinin mixed with citrate-stabilized AuNPs matrix, and (c) bradykinin on AuNPs-PAA substrate.

Besides the analysis of bradykinin peptide, the AuNPs-PAA substrate was also used in the analysis of low molecular weight peptide (glutathione (MW 307.08 g/mol)). As shown in Figure 4.9a, by using CHCA matrix, glutathione is undetectable due to the interference ion peaks from CHCA matrix at low mass region ($m/z \leq 600$). This common phenomenon limits the application of MALDI-MS technique for small molecule detection. Interestingly, when glutathione was analyzed on our developed

modified substrate, it was readily detected without interference peak as shown in Figure 4.9b. There are two dominant peaks in the mass spectrum, which represent $[GSH+H]^+$ (m/z 308) and $[2GSH+H]^+$ (m/z 615). Moreover, the lower laser energy (50% laser 100 shots) was required in the detection on the AuNPs-PAA substrate when compared to the unmodified substrate (using CHCA matrix), indicating the potential of this substrate for low molecular weight compound detection. This newly developed substrate provides an alternative approach for the analysis of small molecules by SALDI-MS technique.

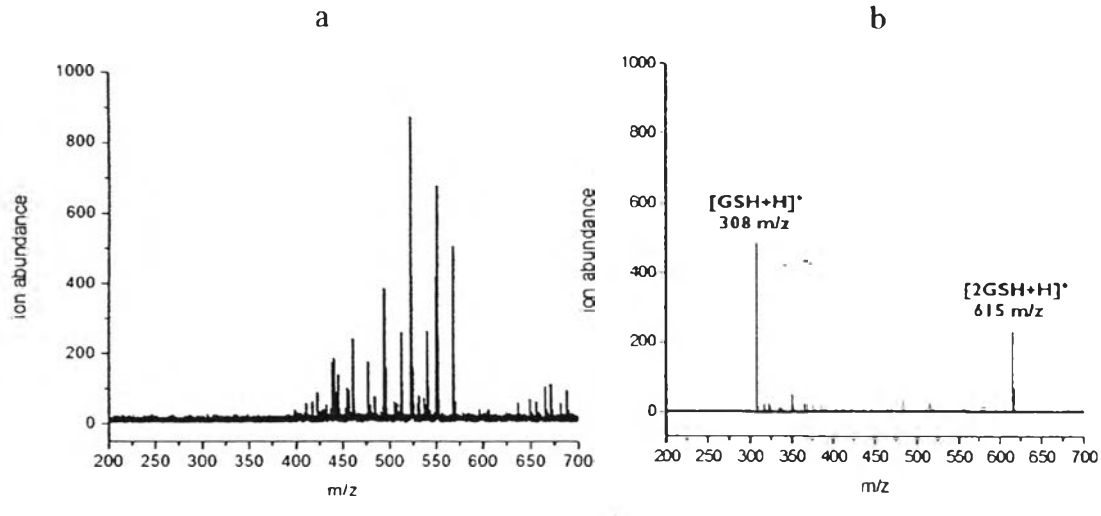

Figure 4.9 Mass spectra of (a) 500 nM glutathione analyzed by using CHCA matrix and (b) 500 nM glutathione analyzed on AuNPs-PAA substrate.

4.3 Selective Detection of Thiol-containing Peptide on AuNPs-PAA Substrate by SALDI-MS.

Due to the strong binding interaction between Au and thiol (-SH) group [33], the selectivity of AuNPs-PAA substrate with thiol-containing peptides (*i.e.* glutathione, ICNKQDCPILE) was investigated. Firstly, a solution mixture of three small molecules

(m/z ≤ 500) which are glutathione (m/z 307.32), sucrose (m/z 342) and cholesterol (m/z 386.65) was incubated and then analyzed on AuNPs-PAA substrate. The result shown in Figure 4.10a indicates that only glutathione was detectable on the modified substrate, which may be explained as a consequence of selective binding between Au on the modified substrate and the thiol group of glutathione. Then, the selectivity of the substrate was further tested with the peptides with higher mass (MW ≥ 1000 g/mol) by using a solution mixture of ICNKQDCPILE (m/z 1274) and bradykinin (m/z 1060.21). As seen in Figure 4.10b, only ICNKQDCPILE that contains thiol group on cysteine unit was selectively detected at m/z of 1275 $[M+H]^+$. This high selectivity of the modified substrate towards thiol-containing peptide is very useful for the applications that require high specificity for the detection of thiol-containing peptides in complex biological samples (*e.g.* human serum, cell lysates).

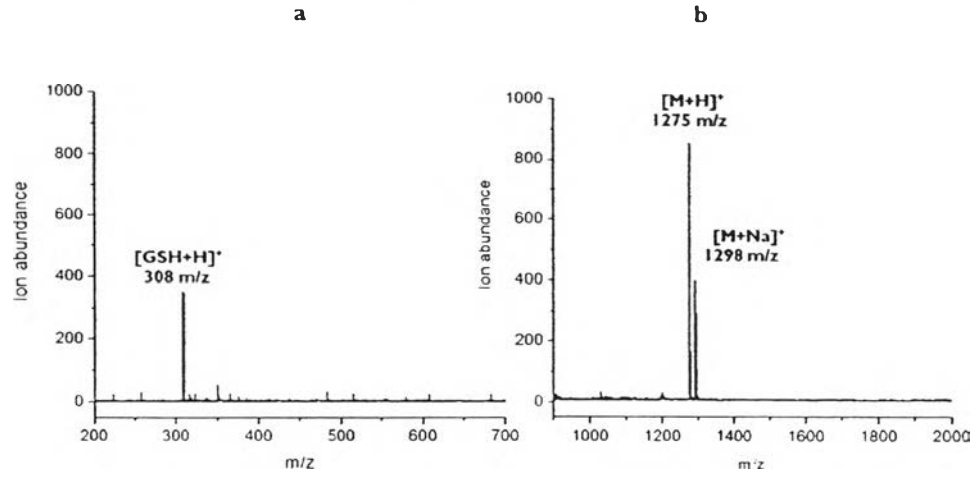

Figure 4.10 Mass spectra of (a) a mixture of 500 nM glutathione, sucrose, cholesterol and (b) a mixture of 500 nM bradykinin and ICNKQDCPILE analyzed on AuNPs-PAA substrate by SALDI-MS.

The detection limit of thiol-containing peptides (glutathione, ICNKQDCPILE) on these substrates were also estimated. As shown in Figure 4.11, the limit of detection (LOD) of glutathione and ICNKQDCPILE were found to be 0.1 nM and 0.05 nM, respectively on AuNPs-PAA substrate. Thus, by using our modified substrate, the thiol-containing peptide can be selectively and sensitively detected without the use of organic matrix.

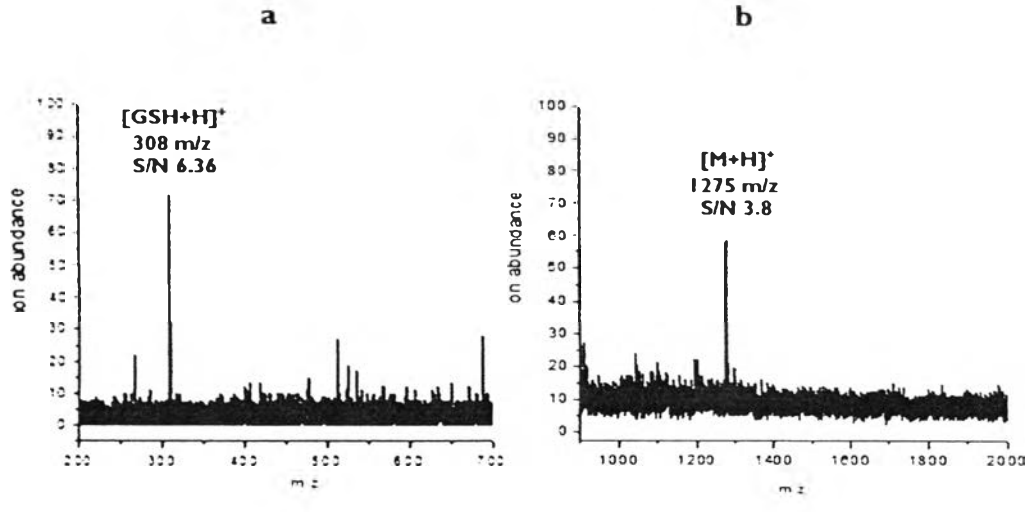

Figure 4.11 Mass spectra of (a) 0.1 nM glutathione and (b) 0.05 nM ICNKQDCPILE analyzed on AuNPs-PAA substrate.